We are IntechOpen,
the world's leading publisher of
Open Access books
Built by scientists, for scientists

6,900
Open access books available

186,000
International authors and editors

200M
Downloads

154
Countries delivered to

Our authors are among the

TOP 1%
most cited scientists

12.2%
Contributors from top 500 universities

BOOK CITATION INDEX
CLARIVATE ANALYTICS
INDEXED

WEB OF SCIENCE™

Selection of our books indexed in the Book Citation Index
in Web of Science™ Core Collection (BKCI)

Interested in publishing with us?
Contact book.department@intechopen.com

Numbers displayed above are based on latest data collected.
For more information visit www.intechopen.com

Noble Metal-Based Nanocomposites for Fuel Cells

Hongpan Rong, Shuping Zhang,
Sajid Muhammad and Jiatao Zhang

Additional information is available at the end of the chapter

Abstract

Noble metal-based nanocomposites are attractive for a rich variety of electrocatalytic applications as they can exhibit not only a combination of the properties associated with each component but also synergy due to a strong coupling between different constituents. Using noble metal as the base component, a plenty of methods have been recently demonstrated for the synthesis of noble metal-based nanocomposites with novel structures (e.g., alloys, core-shell, skin and 1D/2D structures). In this chapter, an account of recent advances of synthetic approaches to noble metal-based nanocomposites with controlled structures, compositions and sizes are reviewed. The relationship between structures and electrochemical properties of these nanocomposites in fuel cell field is discussed. The potential future directions of research in the field are also addressed.

Keywords: noble metal, nanocomposites, electrochemical, fuel cell

1. Introduction

With the global rapid increase of energy demand and the depletion of fossil fuels, research on environment-friendly energy sources has attracted considerable attention in recent years. The real commercialization of fuel cells is a promising solution for the global problems of energy supply and clean environment. A fuel cell can convert chemical energy into electric energy by an electrochemical reaction of hydrogen-containing fuel with oxidant. Based on the electrolyte type, fuel cells are classified to be several kinds: proton exchange membrane fuel cells (PEMFCs), phosphoric acid fuel cells (PAFCs), solid acid fuel cells (SAFCs), alkaline fuel cells (AFCs) and high-temperature fuel cells. Among all kinds of fuel cells, only hydrogen PEMFC has been used in commercial vehicles (the Toyota Mirai) from 2014, due to its short start-up time, high-energy density and low working temperature. Thus, we will focus on PEMFCs in this chapter. Besides hydrogen, other fuels which are suitable for PEMFCs include alcohols (methanol, ethanol, glycol etc.) and formic acid. Compared with hydrogen, they have lower

energy density [1]. But they are cheap, plentiful, easily stored and transported. Therefore, direct methanol fuel cell (DMFC), direct ethanol fuel cell (DEFC), and direct formic acid fuel cell (DFAFC) are also promising in commercial applications.

At the anode of a fuel cell, hydrogen-containing fuel is oxidized to produce electrons that are transferred to the cathode through an external circuit. At the cathode, oxygen is reduced to be water. Thus, catalysts are essential at both electrodes to promote the fuel oxidation reaction and oxygen reduction reaction (ORR). Most fuel oxidation and oxygen reduction reactions catalyzed by noble metal-based nanocomposites are performed in acidic solutions. The reason contains two aspects: (1) for DMFCs, DEFCs and DFAFCs, carbonates can form in alkaline electrolyte [1]; (2) hydrogen oxidation reaction on platinum (Pt) in acid is 2 orders of magnitude quicker than in alkaline electrolytes [2]. When the fuel is hydrogen, the hydrogen oxidation reaction (HOR) rate on Pt is extremely fast, and 0.05 mg cm^{-2} Pt loading at the anode is enough. However, to achieve a desirable catalytic performance, the slow reaction rate of ORR at the cathode even on the best Pt-based catalyst needs much more Pt loading amount (~0.4 mg cm^{-2}) [3]. According to the data reported by Vesborg in 2012, Pt is one of the most expensive metals [4]. The large-scale application of fuel cell technology in transportation field or portable power generation is limited by the high cost of electrode catalysts. Numerous researches have been undertaken to improve the intrinsic activity of electrocatalysts to reduce the noble metal loading of the electrodes without compromising fuel cell performance.

The catalytic activity, selectivity and stability of noble metal-based nanocomposites are closely related to the factors including size, shape/morphology and composition [5–8]. In the past decade, various experimental methods have been developed to synthesize size-dependent, high catalytic performance noble metal-based nanocomposites with diverse morphologies, such as polyhedron, concave, wire, plate, belt/ribbon, dendrite/branch and cage/frame structures [9–21]. Smaller size means higher surface-area-to-volume ratio, higher atomic utilization efficiency and more catalytic active sites. During electrochemical process, small-size noble metal-based nanocomposites provide high electrocatalytic activity, but the challenge is the aggregation that could happen under electrocatalytic conditions, resulting in the poor performance of long-term stability test (e.g., commercial Pt/C). Alloying one or two kinds of transition metals with noble metal has become a valid strategy to develop excellent electrocatalysts [22–25]. The addition of the second/third metal not only changes the surface active sites by ensemble effect, but also alters the binding strength of reactants, intermediates, and products by electronic/strain effect [26–28]. Different noble metals polyhedrons/concave expose atoms with different coordination numbers, thus have different surface energy and exhibit different catalytic performances [29–31]. 1D (wire) and 2D (plate, belt/ribbon) noble metal-based nanostructures have high surface area (high atom utilization efficiency), high conductivity and large interfacial area contacting with the support in electrochemical reactions [12, 15, 32]. Dendrite and branch structures not only exhibit large surface area and high active sites, but also significantly relieve the aggregation happened in electrocatalytic stability test [9, 33, 34]. Highly open noble metal nanocages and nanoframes exhibit enhanced electrocatalytic properties due to their three-dimensional accessible surface atoms [20, 35, 36]. A nanosegregated noble metal skin on these open structures can further improve the catalytic performance [18, 37]. Thus, numerous shape-controlled synthetic

strategies are established in colloidal reaction system, such as facet-selective capping (CO [38, 39], halide anions [40], amines [9], formaldehyde [30, 41], etc.), seed growth [42, 43] and oxidative etching [44].

In this chapter, we focus on the key factors behind the novel synthesis strategies and provide the discussions along the topic of composition. The very recent achievements of the controllable synthesis of noble metal-based nanocomposites are given and discussed on the structure-property relations in electrochemical reactions.

2. Pt-based nanocomposites

At present, owing to the outstanding catalytic activity and superior resistant characteristics to corrosion, Pt-based nanoparticles (NPs) supported on porous carbon are still the most efficient catalysts in PEMFCs [15, 16, 18, 27]. In the past several years, to develop advanced Pt-based nanocatalysts for electrochemical reaction, researchers have proposed several synthesis strategies, which mainly include (1) alloying, (2) core-shell, (3) Pt-skin, (4) 1D or 2D structures and (5) porous, caged, hollow and frame structures. The integration of two or more strategies into one kind of Pt-based nanocomposites is beneficial for the construction of super-electrocatalysts with excellent catalytic activity and stability.

2.1. Pt-based alloys and intermetallics

In the past decade, Pt-based nanostructures have been widely used to prepare excellent catalysts for diverse chemical reactions [45–47]. Compared with pure Pt nanocatalysts, Pt-based alloy and/or intermetallics exhibit higher activity and stability [48]. As since the surface electronic structure and d-band center position of Pt were changed by incorporating a second and/or third metal into Pt lattice. Owing to higher oxidation potentials of transition metals than Pt, they are always removed from the surface of Pt-based alloy by electrochemical leaching. A pure Pt shell with a thickness of more than several atomic layers is produced after the dealloying process [49]. Although the dealloyed Pt-based nanocatalysts show a higher electrochemical activity compared with Pt/C [50], they perform a poor long-term durability since the re-deposition of leached transition metal onto the anode [51].

For bimetallic and multi-metallic Pt-based nanocomposites, the exposed crystal facet has a close relationship with their electrocatalytic performance. Tian et al. and Stamenkovic et al. have demonstrated that the ORR activities on Pt decrease in the order of high-index facet (hkl) > (111) ≫ (100) in $HClO_4$ solution [52]. Well-defined shapes of Pt-based nanocrystals (NCs) are, thus, of great interest for boosting electrochemical performance. It is believed that the surface energy of a fcc Pt NCs exposed with different facets increases in an order of (111) < (100) < (110) < (hkl) [53]. Accordingly, high-energy crystal facets and surface defects vanish quickly during the NC growth process due to the adatom incorporation on them. Therefore, it is a challenge to prepare NCs with high-index facets and high density of surface defects. Compared with alloy, intermetallic compounds show outstanding structure stability owing to the ordered atom arrangements. Rong et al. developed a kinetically controlled

method to tune the surface defect of Pt-based intermetallics [24]. Based on their proposed growth mechanism, large electronegativity difference, etching and diffusing processes are necessary for the synthesis of defect-rich cubic intermetallic Pt_3Sn NCs. In this protocol, N,N-dimethylformamide (DMF) is solvent and poly(vinylpyrrolidone) (PVP) is surfactant. As shown in **Figure 1**, rich surface defects endow the defect-rich cubic Pt_3Sn NCs with excellent catalytic activity for formic acid oxidation reaction, excellent stability caused by the structure stability of intermetallic compounds.

2.2. Ultrathin Pt-based nanocomposites

2.2.1. Ultrathin Pt-based nanowires (NWs)

Ultrathin Pt-based NWs with a diameter of few atomic layers present high ratio of surface atoms to bulk atoms, which could increase Pt utilization efficiency greatly. During the synthesis process of bimetallic and multi-metallic Pt-based NWs, there are two obstacles to overcome: (1) controlling the reduction and nucleation process of different kinds of metal precursors with different reduction potentials; (2) confining the growth along a certain direction and inhibiting the other two directions. While diverse efforts to develop such materials have been made, some achievements of the fabrication of ultrathin Pt-based NWs with few nanometers have been reported. Oleylamine (OAm) was widely used as soft template in the preparation of ultrathin Pt-based NWs. In 2007, Sun's group synthesized ultrathin Pt-Fe NWs with a diameter of 2–3 nm in a mixed solution of 1-octadecene (ODE) and OAm [54]. The length of Pt-Fe NWs ranged from 20 to 200 nm with the tuning volume ratio of OAm/ODE. They claimed that OAm self-organizes into reverse-micelle-like structure in ODE solution and higher ratio of OAm/ODE resulted in the formation of longer NWs.

In the same OAm/ODE system, Li et al. prepared Pt/NiO core-shell NW first, subsequently reduced it into PtNi alloy NWs by thermal annealing and finally converted it into jagged Pt NWs through electrochemical dealloying (**Figure 2**). The jagged Pt NWs had shorter Pt—Pt bond length than regular Pt NWs and/or bulk Pt. Short Pt—Pt bond length resulted in a compressive strain on the surface, which produced the world record ORR properties. The specific and mass activity for ORR at 0.9 V vs. reversible hydrogen electrode (RHE) are 11.5 mA cm^{-2} and 13.9 A/mg$_{Pt}$, respectively [16].

As shown in **Figure 2**, Huang's group used OAm as the solvent, reductant and surfactant, cetyltrimethylammonium chloride (CTAC) as structure-directing and glucose as reducing reagent to synthesize hierarchical platinum-cobalt (Co) NWs [14]. These PtCo NWs had high-index, Pt-rich facets and ordered intermetallic structure. The novel structure enabled the PtCo NWs excellent performance toward alcohol oxidation reactions and ORR (39.6/33.7 times of the specific/mass activities than commercial Pt/C for ORR). They used CTAC, Mo(CO)$_6$ and Ni(acac)$_2$ (acac = acetylacetonate) as structure-directing reagent to prepare subnanometer Pt NWs with a diameter of 0.8 nm [17]. They claimed that the carbonyl decomposed from Mo(CO)$_6$, Ni^{2+} and proper amount of CTAC were important for the formation of 1D structure. With addition of a stronger reductant (glucose), they fabricated PtNi, PtCo and PtNiCo NWs with similar diameter. These subnanometer Pt alloy NWs showed enhanced ORR activity and stability (mass and specific activities of 4.20 A mg$_{Pt}$ and 5.11 mA cm^{-2} at 0.9 V vs. RHE). They
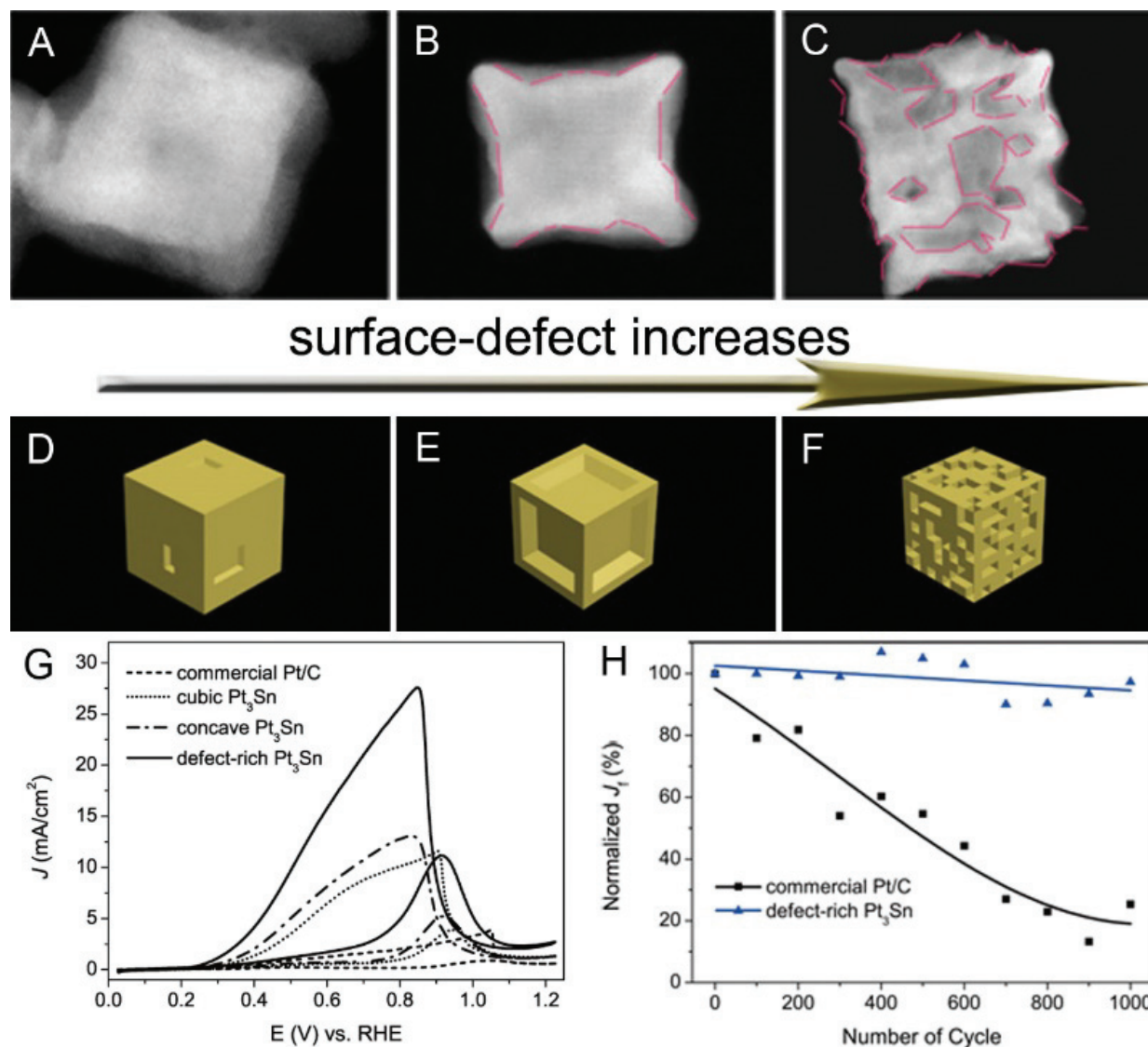
Figure 1. (A–C) HAADF-STEM images and (D–F) corresponding structure model of (A and D) cubic, (B and E) concave cubic, and (C and F) defect-rich cubic intermetallic Pt_3Sn NCs. (G) Cyclic voltammograms of formic acid oxidation in 0.1 M $HClO_4$ + 1 M HCOOH (scan rate: 50 mV/s). (H) Loss of peak current density in forward scans as a function of cycling numbers (0.65–1.23 V vs. RHE, scan rate: 50 mV/s). Reprinted with permission from Ref. [24]. Copyright 2016 Wiley-VCH Verlag GmbH & Co. KGaA, Weinheim.

used this effective reaction system to synthesize a series of Pt-based NWs for electrochemical reactions: (1) PtNiPd core-shell NWs showed superior glycoloxidation reaction (EGOR), glycerol oxidation reaction (GOR) and ORR performances [55], (2) porous Pt_3Ni NWs with extraordinary catalytic performance toward methanol oxidation reaction (MOR) and ORR [56], (3) hierarchical PtPb NWs exhibited higher activity and stability for MOR and ethanol oxidation reaction (EOR) than commercial Pt/C [57], (4) screw thread-like PtCu NWs showed excellent properties for MOR and EOR [58].

Recently, Li's group realized the reduction of Mo in this reaction system by a hydrogen assisted solution route (HASR) [32]. Ultrathin Pt-Mo-Ni NWs with a diameter of ~2.5 nm were
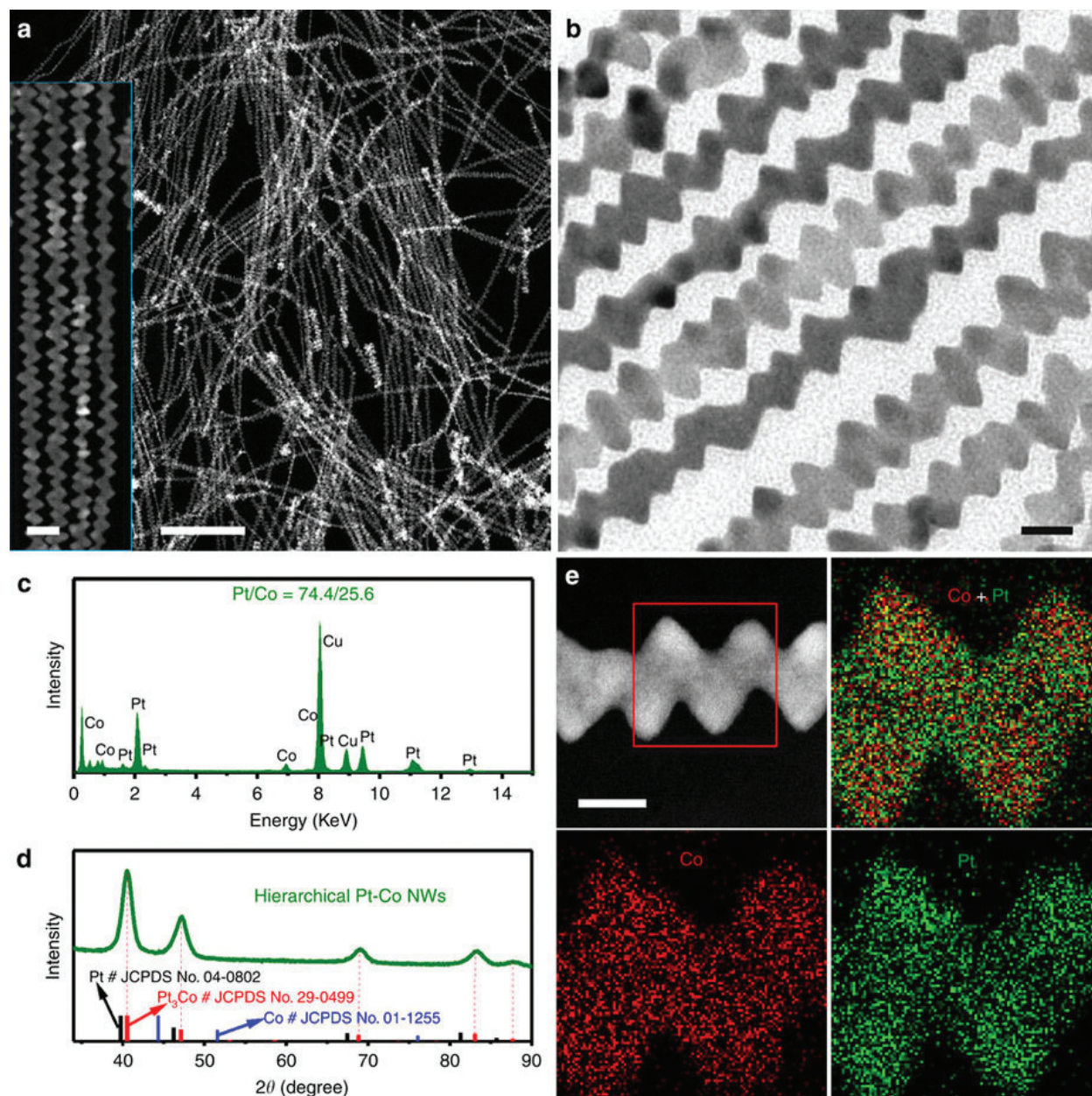
Figure 2. Representative (a) STEM image, (b) TEM image, (c) TEM-EDS, (d) PXRD pattern and (e) STEM-ADF image and EDS elemental mappings of the hierarchical Pt₃Co NWs. Inset in (a) is an enlarged STEM image. The composition is Pt/Co = 74.8/25.2, as revealed by ICP-AES. The scale bars in (a), inset of (a), (b) and (e) are 200, 20, 10 and 10 nm, respectively. Reprinted with permission from Ref. [14]. Copyright 2016 Nature Publishing Group.

successful synthesized in OAm. Hydrogen served not only as reductant, but also as structure-directing species. A series of Pt-Mo-M (M = Fe, Co, Mn, Ru) NWs could be synthesized by this HASR method. The Pt-Mo-Ni NWs exhibited higher maximum power density than Pt/C in DEFC experiments.

In the above mentioned cases, soft template method is very effective in OAm system to construct ultrathin Pt-based NWs. The largest extent exposure of Pt atoms results in the extraordinary electrochemical activity. The presence of the second and third transition metal

can not only relieve the undesirable overbinding of oxygen atoms on catalyst, but also stabilize the undercoordinated active sites, further improving the electrochemical activity and stability. While the synthesis of ultrathin Pt-based NWs has many achievements, more innovative works are still desired to enrich this field.

2.2.2. Core-shell structures with ultrathin Pt shell

Since catalytic reactions take place on the surface of nanocatalysts, the alteration of surface composition and electronic structure directly causes different catalytic properties [59]. The physical and chemical properties of core-shell nanostructures can be altered by the design of core, shell and interface. The construction of Pt shell on the surface of nanocatalysts is another possible solution to prepare enhanced Pt-based catalysts with minimum usage of Pt. The catalytic properties of Pt based core-shell NCs have close relationship with the Pt shell thickness. The charge transfer between core and shell components changes the band structure of shell, thus influencing the catalytic performance [60]. The electronic and geometric properties of the top surface layer are affected by the core, and the influence decreases with the increased thickness of shell. For core-shell structures with thin shell, the different lattice constant between core and shell components results in the lattice strain and brings geometric effect [61]. Strong electrochemical activity enhancements have been observed for monolayer or a few atomic layer Pt shells. Thanks to the development of instrumental techniques, researchers can study ultrathin Pt shells closely and clearly.

So far, diverse synthetic strategies have been developed to prepare diverse inorganic core-shell structures: semiconductor@semiconductor [62], metal@metal [63, 64], semiconductor@metal [65], metal@semiconductor [66–68], and even multishell structures [69].

Several synthetic strategies have been developed to fabricate core-shell structures, such as seed-mediated growth, dealloying, galvanic replacement and one-pot synthesis. The most effective and widely used synthetic methodology is seed-mediated growth. Adzic and co-workers have fabricated various core-shell electrocatalysts with monolayer and ultrathin Pt shell via Cu under potential deposition (UPD) and pulse electrodeposition (PED). The core materials contain intermetallics (PtPb, PdPb, PdFe) [70], core-shell (Pd@PdAu) [71], alloy (AuNi) [72] and transition metal nitride (TiCuN) [73]. As shown in **Figure 3**, in an UPD process, they prepared core first, then dropped onto a flat glassy electrode to form a thin film. The electrodes were deposited Cu monolayer in a H_2SO_4 + $CuSO_4$ solution, then rinsed in a K_2PtCl_4 + H_2SO_4 solution to replace Cu with Pt. The Cu deposition and replacement operations were conducted under an Ar atmosphere [70]. Due to the limited electrode area and critical synthesis conditions, UPD and PED are not suitable for the large-scale preparation of core-shell nanocatalysts with ultrathin Pt shell. Zhang's group reported the synthesis of Ag@Pt and Au@Ag@Pt particles with a controllable thin Pt shell by interface-mediated galvanic replacement. These sub-ten-nanometer core-shell NCs showed better ORR performance than Ag [74].

Utilizing the different reduction potentials of different metal precursors, bimetallic core-shell structure could be prepared by one-pot synthetic process [75, 76]. However, it is still a challenge to control this process since alloys or heterostructures with uncontrolled morphologies are usually produced. Bu et al. synthesized PtPb@Pt core-shell nanoplate in OAm/ODE mixture and this
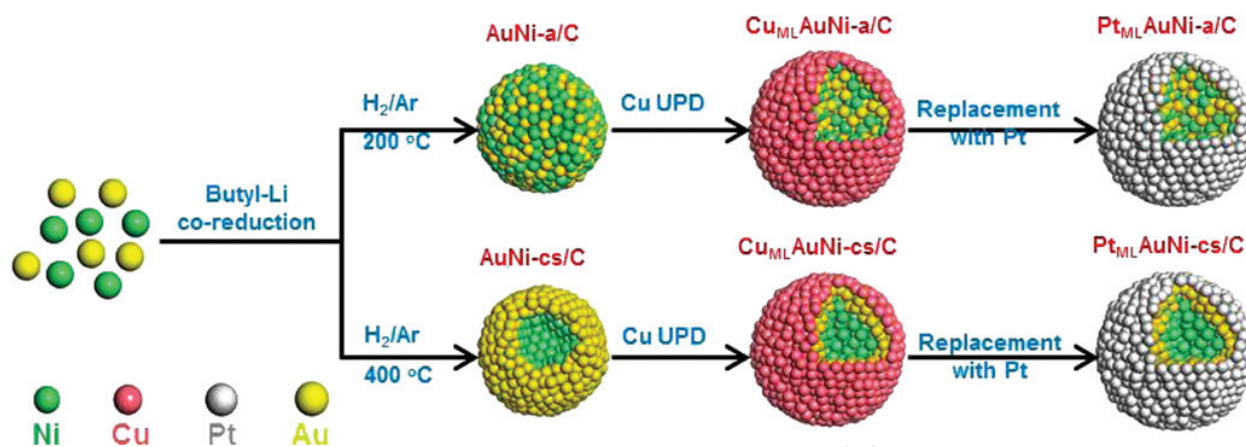
Figure 3. Schematic illustration of the stepwise synthesis of monolayer Pt core-shell electrocatalysts. Reprinted with permission from Ref. [72]. Copyright 2016 American Chemistry Society.

nanoplate exhibited about eight-fold increase in mass activity for MOR and EOR and enhanced ORR performance compared with Pt catalyst. In their synthesis process, L-ascorbic acid was used as the reducing reagent. The Pt shell thickness was 0.8–1.2 nm (equal to four to six atomic layers). According to the well-established *d*-band model, tensile lattice strain upshifts the *d*-band center and thus results in a stronger bonding with adsorbates and a lower reaction rate. In the case of PtPb@Pt core-shell nanoplate, although Pb atom in the core is larger than Pt, the tensile strain did not decrease the electrochemical properties. They claimed that the surface strain effect on binding behavior was facet dependent, and the tensile strain on the exposed Pt(110) helped to decrease the Pt—O bond strength.

Compared to monolayer Pt shell, a few atomic layer Pt shell can protect the transition metal atoms from leaching under electrochemical operation and have better stability. However, the stability of core-shell structured nanocatalysts with ultrathin Pt shell is still far away from satisfactory.

3. Other noble metal-based nanocomposites

3.1. Pd-based nanocomposites

Palladium (Pd)-based nanocomposites have exhibited extraordinary performance in diverse applications such as hydrogenation reactions [5, 77], photothermal therapy [78], cross-coupling reactions [79] and electrochemical reactions [80–82]. Pd and Pt are in the same group and Pd-Pt nanostructures have showed excellent electrocatalytic properties [37, 83]. Considering Pt-based nanocomposites that have been discussed above, Pd-Pt nanostructures are not reviewed in this subsection.

The electrochemical reactions on Pd NCs are structure sensitive. For the low index planes of Pd, Kondo et al. reported that reduction current density of ORR at 0.9 V (RHE) increased in the order of (110) < (111) < (100) [84]. Shao et al. also demonstrated that the specific activity of Pd nanocubes exposed with {100} facets was about 10 times higher than that of Pd octahedral

enclosed with {111} facets toward ORR [85]. Compared with hydrophilic solvents such as water, ethylene glycol and DMF, systematic shape control of Pd NCs in hydrophobic solvent remains a challenging task. As shown in **Figure 4**, Niu et al. synthesized icosahedral, decahedral, octahedral, tetrahedral and triangular plates Pd NCs in the mixture of OAm, formaldehyde and toluene [30]. In this protocol, Pd(acac)$_2$ was used as the metal precursor and the morphology of Pd was determined by the quantity of OAm. Different intermediates were formed with different amount of OAm under room temperature stirring and reduction rate decreased with the increase amount of OAm. Seeds were formed with the addition of formaldehyde at room temperature, which also acted as selective surfactant in this reaction
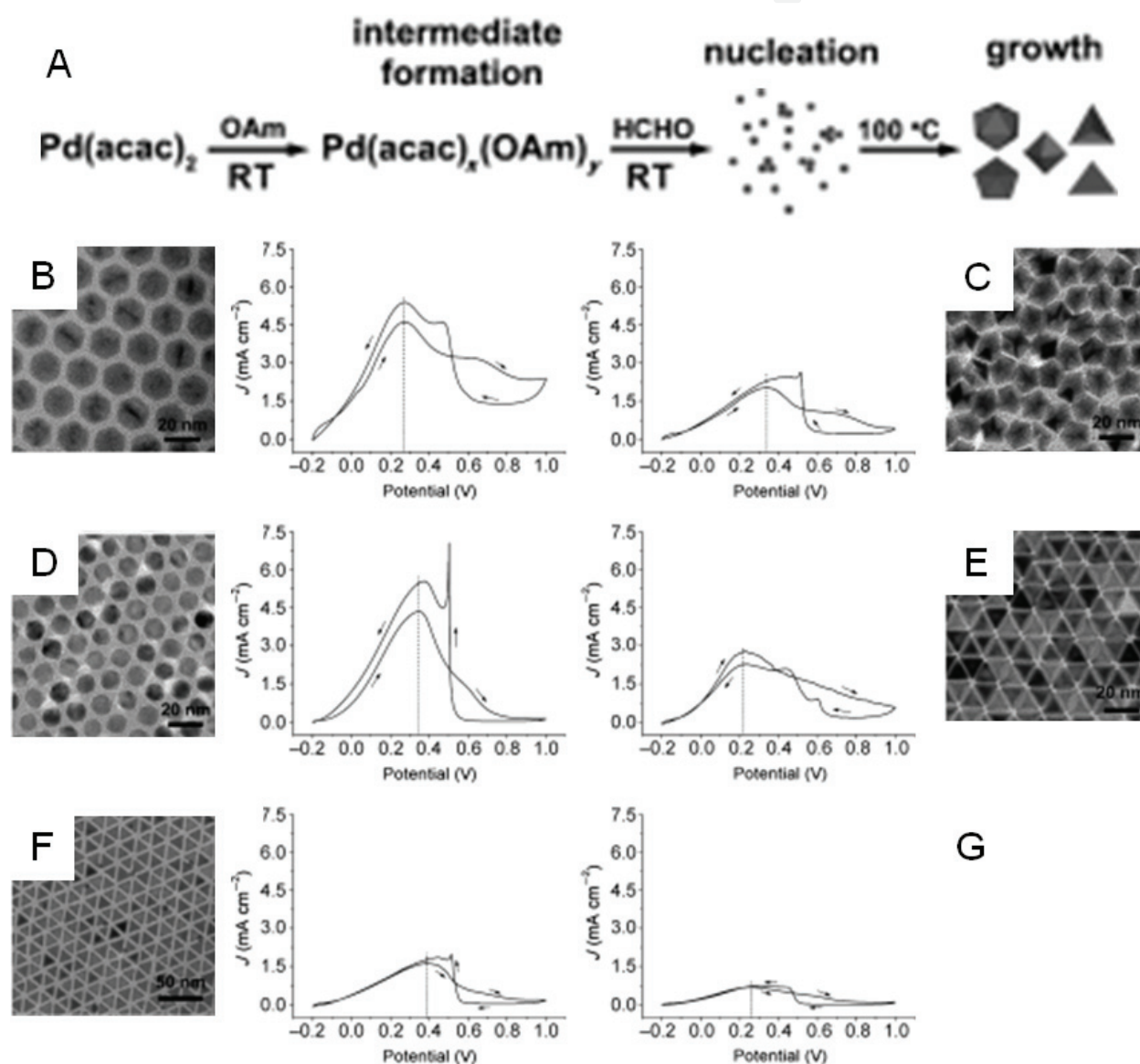

Figure 4. (A) Proposed mechanism for formation of Pd NCs. (B–F) TEM images and (B–G) cyclic voltammograms of Pd catalysts with different shapes in 0.1 M HClO$_4$ and 2 M HCOOH solution at a scan rate of 50 mV s^{-1}. (B) Icosahedral Pd, (C) decahedral Pd, (D) octahedral Pd, (E) tetrahedral Pd, (F) triangular platelike Pd, and (G) commercial Pd. Adapted with permission from Ref. [30]. Copyright 2011 Wiley-VCH Verlag GmbH & Co. KGaA, Weinheim.

system. Growth process was observed at elevated temperature and the final morphology was decided by the co-action of surface energy, elastic strain energy and twin boundary energy. The maximum current densities of the prepared Pd NCs were in the order of icosahedral ≈octahedral > tetrahedral > decahedral > triangular plates toward formic acid oxidation reaction.

Among bimetallic Pd-base nanocatalysts for electrochemical reactions, PdCu NCs have received a great deal of attention due to the low cost and good performance. Yin et al. prepared PdCu NPs by emulsion-assisted ternary ethylene glycol system, which showed superior methanol oxidation activity than Pd in alkaline solution [86]. Mao et al. also synthesized PdCu NCs with tunable compositions in octadecylamine. $Pd_{0.5}Cu_{0.5}$ exhibited the highest mass activity for ethanol electro-oxidation in alkaline solution [8]. Gao et al. prepared PdCu nanocubes in OAm and the PdCu nanocubes showed 2 times mass activity than commercial Pt/C catalysts [87].

Although numerous Pd-based nanocomposites have been proven to show excellent electrocatalytic activities, but the stability is still a major issue for Pd-based electrocatalysts even in alkaline solution. Better performance of Pd-based nanocomposites is essential for the substitute of Pt in the application of fuel cell.

3.2. Other noble metal-based nanocomposites

Generally speaking, besides Pt and Pd, noble metals also contain gold (Au), silver (Ag), rhodium (Rh), ruthenium (Ru), osmium (Os) and iridium (Ir). They are always used to modify the electronic structure of Pd and Pt in the fuel cell application and these nanocomposites will not be discussed below [88–92].

Since Haruta et al. reported the oxidation of CO by supported Au at low temperature, Au-based nanocomposites have received a great deal of attention in catalytic field [93]. Surfactants being on the surface may decrease the electrochemical activities. Yin et al. used reduced grapheme oxide (rGO) as reductant and support to confine the growth of Au so they prepared surfactant-free Au/rGO hybrids for ORR in alkaline solution [94]. In this method, utilizing the electrostatic interaction between negative-charged rGO and positive Au(III) ions also the coordination effects between heteroatoms at the defects of rGO and Au(III) ions, Au clusters with a diameter of 1.8 nm were reduced and anchored by rGO. Although the catalytic activity was not as good as Pt/C, Au/rGO exhibited relatively high onset potential, methanol tolerance, and extraordinary stability (**Figure 5**).

By introducing other metal components, the cost of Au can be reduced, the modification of crystallography and electronic structure may increase the catalytic performance. With abundant tip, edge and surface atoms, 2D Au-based nanocomposites have attracted increasing attention. Xu et al. prepared AuCu bimetallic NCs with tunable composition via a simple wet-chemical method [95]. The 2D AuCu triangular porous nanoprisms exhibited high electrocatalytic activity. The mass activities of Au_1Cu_1 for ethylene glycol and glycerol electrooxidation reactions were 3.0- and 3.9-fold improvements over those of pure Au, respectively.

Owing to the poor stability in acidic solution, ORR catalyzed by Ag was always demonstrated in alkaline solution [96, 97]. Tammeveski et al. prepared the Ag-based nanocomposites by sputter deposition of Ag on the surface of multi-walled carbon nanotube [96]. They analyzed
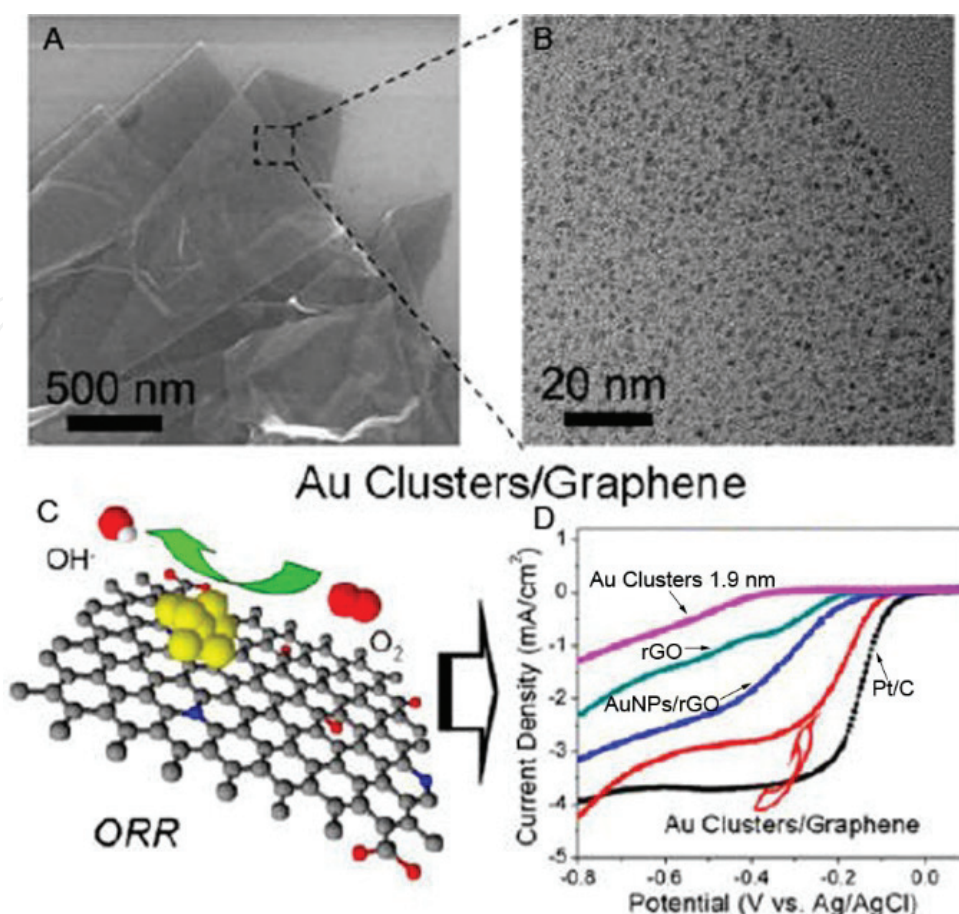
Figure 5. (A) SEM, (B) TEM images of as-prepared Au/rGO hybrids. (C) Scheme of the ORR happened on Au/rGO hybrids. (D) RDE curves of commercial Pt/C, Au/rGO hybrids, Au NP/rGO hybrids, rGO sheets, Au clusters in O_2-saturated 0.1 M KOH at a scanning rate of 50 mV/s at 1600 rpm. Reprinted with permission from Ref. [94] Copyright 2012 American Chemistry Society.

rotating disk electrode (RDE) data by Koutecky-Levich equation and demonstrated that O_2 was reduced by a four-electron pathway. Gupta et al. studied the influence of anisotropic Ag on ORR activity in alkaline media [97]. They prepared Ag NPs in ethylene glycol with different ratio of anisotropic NPs by adding different amount of $Cu(CH_3COO)_2 \cdot H_2O$, which acted as etchant. They reported that sample containing higher ratio of anisotropic Ag NPs showed better ORR performance.

Zheng et al. studied the size effect of Ir/C toward hydrogen oxidation/evolution reaction (HOR/HER) in alkaline solution [98]. They prepared Ir/C with different sizes by heat treating commercial Ir/C at different temperature. Higher temperature resulted in larger size. The particle sizes of Ir/C changed from 3 to 12 nm. Different from the law of Pt NCs with the same size range, larger Ir/C had higher HOR/HER activities. Qin et al. utilized CeO_2 and C to disperse Ir NPs; the mass and specific activities of Ir/CeO_2-C toward HOR in alkaline conditions are 2.8- and 1.8-fold higher than Ir/C. They claimed that the addition of CeO_2 decreased the agglomeration extent of Ir NPs, and the particle size changed from 1.1 to 3.4 nm after 2000 potential cycles [99].

Lin et al. reported a salt-templated method to prepare Rh (1.6 nm)/ultrathin carbon nanosheets, which displayed a comparable ORR activity and better durability to commercial Pt/C under basic conditions [100]. The salt template was green and easy to remove. In this approach, Na_2SO_4 particles acted as template and poured into prefabricated rhodium oleate. During the subsequent heat-treatment under N_2, Rh NPs were reduced and anchored on the ultrathin carbon nanosheets transformed from oleate. After water rinsing, Na_2SO_4 particles were removed and Rh/ultrathin carbon nanosheets were obtained.

Owing to the strong Ru—O bond strength, metallic Ru show poor ORR activity. The addition of Se can transfer charge from Ru to Se, which reduces the oxygen binding energy on Ru and increases the ORR activity [3]. Cao et al. prepared Se-modified Ru NPs by heating the Ru black and Se in xylene under refluxing condition with Ar bubbling [101]. The ORR activity of Se-modified Ru NPs in H_2SO_4 was higher than that of clean and Se-modified Ru disk. Zaikovskii et al. fabricated Se-modified Ru/C by reacting Ru/C NPs with SeO_2 followed by annealing [102]. They prepared RuSe/C with different Se coverage by tuning the ratio of Se/Ru. Higher amount of Se caused lower extent of Ru oxidation, thus resulting in higher ORR activity. However, Ru is the active center for ORR and blocked shell of RuSe decreased ORR activity. Neergat et al. synthesized RuSe NPs by reducing $RuCl_3 \cdot xH_2O$ and SeO_2 by $NaBH_4$ in water at 80°C [103]. They investigated the ORR performance of several nanocatalysts in the presence of methanol, and the ORR activities were in the order of Ir < Pt < Rh < IrSe < RhSe < RuSe.

4. Conclusions and outlooks

This chapter has demonstrated the significant developments that have been accomplished in the noble metal-based nanocomposites for fuel cell. For the past decade, great progress has been made in developing Pt- and Pd-based nanocomposites for electrochemical reactions in fuel cell. Surface electronic structure of Pt and Pd can be modified by incorporating a second and/or third metal, which significantly influences the electrochemical performance. Constructing Pt ultrathin structure is an effective strategy to improve the utilization of Pt and the specific activity of Pt-based nanocatalysts. Significant progresses have been made on Ir-, Rh-, and Ru-based nanocatalysts. However, their activities are still not comparable to those of Pt- and Pd-based catalysts, especially those of Pt-based nanocomposites. For the practical application, fuel cell is still a long way to go.

At present, most Pt-based catalysts are characterized by RDE technique, which is a fast screening technique. They need to be evaluated in a fuel cell environment before large-scale application. As a result, simple preparation method is very important for scale production of catalysts. Wet-chemical method is suitable for scale preparation. Researchers need to optimize the fabrication technology of the state-of-the-art noble metal-based electrocatalysts, and find a simple, green and low-cost preparation method. Developing in situ characterization technique for the electrochemical process will provide a basis for mechanism exploration. According to the excellent catalytic performance of binary noble metal structures, general preparation strategies and catalytic property studies for tri- and multi-metallic nanocomposites are urgent.

Author details

Hongpan Rong, Shuping Zhang, Sajid Muhammad and Jiatao Zhang*

*Address all correspondence to: zhangjt@bit.edu.cn

Beijing Key Laboratory of Construction-Tailorable Advanced Functional Materials and Green Applications, School of Materials, Beijing Institute of Technology, Beijing, PR China

References

[1] Kakati N, Maiti J, Lee SH. Anode catalysts for direct methanol fuel cells in acidic media: Do we have any alternative for Pt or Pt-Ru? Chemical Reviews. 2014;**114**:12397-12429. DOI: 10.1021/cr400389f

[2] Elbert K, Hu J, Ma Z. Elucidating hydrogen oxidation/evolution kinetics in base and acid by enhanced activities at the optimized Pt shell thickness on the Ru core. ACS Catalysis. 2015;**5**:6764-6772. DOI: 10.1021/acscatal.5b01670

[3] Shao M, Chang Q, Dodelet J-P. Recent advances in electrocatalysts for oxygen reduction reaction. Chemical Reviews. 2016;**116**:3594-3657. DOI: 10.1021/acs.chemrev.5b00462

[4] Vesborg PCK, Jaramillo TF. Addressing the terawatt challenge: Scalability in the supply of chemical elements for renewable energy. RSC Advances. 2012;**2**:7933-7947. DOI: 10.1039/c2ra20839c

[5] Rong H, Cai S, Niu Z. Composition-dependent catalytic activity of bimetallic nanocrystals: AgPd-catalyzed hydrodechlorination of 4-chlorophenol. ACS Catalysis. 2013;**3**:1560-1563. DOI: 10.1021/cs400282a

[6] Rong H, Niu Z, Zhao Y. Structure evolution and associated catalytic properties of PtSn bimetallic nanoparticles. Chemistry—A European Journal. 2015;**21**:12034-12041. DOI: 10.1002/chem.201501442

[7] Cai S, Rong H, Yu X. Room temperature activation of oxygen by monodispersed metal nanoparticles: Oxidative dehydrogenative coupling of anilines for azobenzene syntheses. ACS Catalysis. 2013;**3**:478-486. DOI: 10.1021/cs300707y

[8] Mao J, Liu Y, Chen Z. Bimetallic Pd-cu nanocrystals and their tunable catalytic properties. Chemical Communications. 2014;**50**:4588-4591. DOI: 10.1039/c4cc01051e

[9] Niu Z, Wang D, Yu R. Highly branched Pt-Ni nanocrystals enclosed by stepped surface for methanol oxidation. Chemical Science. 2012;**3**:1925-1929. DOI: 10.1039/c2sc00004k

[10] Ge J, He D, Chen W. Atomically dispersed Ru on ultrathin Pd nanoribbons. Journal of the American Chemical Society. 2016;**138**:13850-13853. DOI: 10.1021/jacs.6b09246

[11] Wu Y, Cai S, Wang D. Syntheses of water-soluble octahedral, truncated octahedral, and cubic Pt-Ni nanocrystals and their structure-activity study in model hydrogenation reactions. Journal of the American Chemical Society. 2012;**134**:8975-8981. DOI: 10.1021/ja302606d

[12] Bu L, Ding J, Guo S. A general method for multimetallic platinum alloy nanowires as highly active and stable oxygen reduction catalysts. Advanced Materials. 2015;**27**:7204. DOI: 10.1002/adma.201502725

[13] Liu H, An W, Li Y. In situ probing of the active site geometry of ultrathin nanowires for the oxygen reduction reaction. Journal of the American Chemical Society. 2015;**137**:12597-12609. DOI: 10.1021/jacs.5b07093

[14] Bu L, Guo S, Zhang X. Surface engineering of hierarchical platinum-cobalt nanowires for efficient electrocatalysis. Nature Communications. 2016;**7**. DOI: 10.1038/ncomms11850

[15] Bu L, Zhang N, Guo S. Biaxially strained PtPb/Pt core/shell nanoplate boosts oxygen reduction catalysis. Science. 2016;**354**:1410-1414. DOI: 10.1126/science.aah6133

[16] Li M, Zhao Z, Cheng T. Ultrafine jagged platinum nanowires enable ultrahigh mass activity for the oxygen reduction reaction. Science. 2016;**354**:1414-1419. DOI: 10.1126/science.aaf9050

[17] Jiang K, Zhao D, Guo S. Efficient oxygen reduction catalysis by subnanometer Pt alloy nanowires. Science Advances. 2017;**3**. DOI: 10.1126/sciadv.1601705

[18] Chen C, Kang Y, Huo Z. Highly crystalline multimetallic nanoframes with three-dimensional electrocatalytic surfaces. Science. 2014;**343**:1339-1343. DOI: 10.1126/science.1249061

[19] He DS, He D, Wang J. Ultrathin icosahedral Pt-enriched nanocage with excellent oxygen reduction reaction activity. Journal of the American Chemical Society. 2016;**138**:1494-1497. DOI: 10.1021/jacs.5b12530

[20] Ding J, Zhu X, Bu L. Highly open rhombic dodecahedral PtCu nanoframes. Chemical Communications. 2015;**51**:9722-9725. DOI: 10.1039/c5cc03190g

[21] Wu Y, Wang D, Zhou G. Sophisticated construction of Au islands on Pt-Ni: An ideal trimetallic nanoframe catalyst. Journal of the American Chemical Society. 2014;**136**:11594-11597. DOI: 10.1021/ja5058532

[22] Wang D, Zhao P, Li Y. General preparation for Pt-based alloy nanoporous nanoparticles as potential nanocatalysts. Scientific Reports. 2011;**1**. DOI: 10.1038/srep00037

[23] Mao J, Chen Y, Pei J. Pt-M (M = Cu, Fe, Zn, etc.) bimetallic nanomaterials with abundant surface defects and robust catalytic properties. Chemical Communications. 2016;**52**:5985-5988. DOI: 10.1039/c6cc02264b

[24] Rong H, Mao J, Xin P. Kinetically controlling surface structure to construct defect-rich intermetallic nanocrystals: effective and stable catalysts. Advanced Materials. 2016;**28**:2540. DOI: 10.1002/adma.201504831

[25] Yu X, Li L, Su Y. Platinum-copper nanoframes: One-pot synthesis and enhanced electro-catalytic activity. Chemistry—A European Journal. 2016;**22**:4960-4965. DOI: 10.1002/chem.201600079

[26] Liu H-l, Nosheen F, Wang X. Noble metal alloy complex nanostructures: Controllable synthesis and their electrochemical property. Chemical Society Reviews. 2015;**44**:3056-3078. DOI: 10.1039/c4cs00478g

[27] Huang X, Zhao Z, Cao L. High-performance transition metal-doped Pt3Ni octahedra for oxygen reduction reaction. Science. 2015;**348**:1230-1234. DOI: 10.1126/science.aaa8765

[28] Bu L, Shao Q, Bin E. PtPb/PtNi intermetallic core/atomic layer shell octahedra for efficient oxygen reduction electrocatalysis. Journal of the American Chemical Society. 2017;**139**:9576-9582. DOI: 10.1021/jacs.7b03510

[29] Liu X, Wang W, Li H. One-pot protocol for bimetallic Pt/Cu hexapod concave nanocrystals with enhanced electrocatalytic activity. Scientific Reports. 2013;**3**. DOI: 10.1038/srep01404

[30] Niu Z, Peng Q, Gong M. Oleylamine-mediated shape evolution of palladium nanocrystals. Angewandte Chemie-International Edition. 2011;**50**:6315-6319. DOI: 10.1002/anie.201100512

[31] Wu B, Zheng N. Surface and interface control of noble metal nanocrystals for catalytic and electrocatalytic applications. Nano Today. 2013;**8**:168-197. DOI: 10.1016/j.nantod.2013.02.006

[32] Mao J, Chen W, He D. Design of ultrathin Pt-Mo-Ni nanowire catalysts for ethanol electrooxidation. Science Advances. 2017;**3**. DOI: 10.1126/sciadv.1603068

[33] Wang W, Wang D, Liu X. Pt-Ni nanodendrites with high hydrogenation activity. Chemical Communications. 2013;**49**:2903-2905. DOI: 10.1039/c3cc40503f

[34] Nosheen F, Zhang Z, Xiang G. Three-dimensional hierarchical Pt-Cu superstructures. Nano Research. 2015;**8**:832-838. DOI: 10.1007/s12274-014-0565-1

[35] Ding J, Bu L, Guo S. Morphology and phase controlled construction of Pt-Ni nano-structures for efficient electrocatalysis. Nano Letters. 2016;**16**:2762-2767. DOI: 10.1021/acs.nanolett.6b00471

[36] Shan A, Cheng M, Fan H. NiPt hollow nanocatalyst: Green synthesis, size control and electrocatalysis. Progress in Natural Science-Materials International. 2014;**24**:175-178. DOI: 10.1016/j.pnsc.2014.03.013

[37] Zhang Y, Bu L, Jiang K. Concave Pd-Pt core-shell nanocrystals with ultrathin Pt shell feature and enhanced catalytic performance. Small. 2016;**12**:706-712. DOI: 10.1002/smll.201502755

[38] Huang X, Tang S, Mu X. Freestanding palladium nanosheets with plasmonic and catalytic properties. Nature Nanotechnology. 2011;**6**:28-32. DOI: 10.1038/nnano.2010.235

[39] Dai Y, Mu X, Tan Y. Carbon monoxide-assisted synthesis of single-crystalline Pd tetra-pod Nanocrystals through hydride formation. Journal of the American Chemical Society. 2012;**134**:7073-7080. DOI: 10.1021/ja3006429

[40] Xiong Y, Cai H, Wiley BJ. Synthesis and mechanistic study of palladium nanobars and nanorods. Journal of the American Chemical Society. 2007;**129**:3665-3675. DOI: 10.1021/ja0688023

[41] Duan H, Yan N, Yu R. Ultrathin rhodium nanosheets. Nature Communications. 2014;**5**. DOI: 10.1038/ncomms4093

[42] Xia X, Zeng J, McDearmon B. Silver nanocrystals with concave surfaces and their optical and surface-enhanced Raman scattering properties. Angewandte Chemie International Edition. 2011;**50**:12542-12546. DOI: 10.1002/anie.201105200

[43] Mahmoud A, Tabor CE, El-Sayed MA. A new catalytically active colloidal platinum nanocatalyst: The multiarmed nanostar single crystal. Journal of the American Chemical Society. 2008;**130**:4590-4591. DOI: 10.1021/ja710646t

[44] Wu Y, Wang D, Niu Z. A strategy for designing a concave Pt-Ni alloy through controllable chemical etching. Angewandte Chemie-International Edition. 2012;**51**:12524-12528. DOI: 10.1002/anie.201207491

[45] Bai Q, Li D, He L. Solvent-free selective hydrogenation of o-chloronitrobenzene to o-chloroaniline over alumina supported Pt nanoparticles. Progress in Natural Science: Materials International. 2015;**25**:179-184. DOI: https://doi.org/10.1016/j.pnsc.2015.05.005

[46] Lin L, Zhou W, Gao R. Low-temperature hydrogen production from water and methanol using Pt/alpha-MoC catalysts. Nature. 2017;**544**:80. DOI: 10.1038/nature21672

[47] Li N, Tang S, Meng X. Preparation of Pt-GO composites with high-number-density Pt nanoparticles dispersed uniformly on GO nanosheets. Progress in Natural Science-Materials International. 2016;**26**:139-144. DOI: 10.1016/j.pnsc.2016.03.011

[48] Wu J, Yang H. Platinum-based oxygen reduction electrocatalysts. Accounts of Chemical Research. 2013;**46**:1848-1857. DOI: 10.1021/ar300359w

[49] Gan L, Heggen M, Rudi S. Core–shell compositional fine structures of dealloyed PtxNi1–x nanoparticles and their impact on oxygen reduction catalysis. Nano Letters. 2012;**12**:5423-5430. DOI: 10.1021/nl302995z

[50] Koh S, Strasser P. Electrocatalysis on bimetallic surfaces: Modifying catalytic reactivity for oxygen reduction by voltammetric surface dealloying. Journal of the American Chemical Society. 2007;**129**:12624-12625. DOI: 10.1021/ja0742784

[51] Neyerlin KC, Srivastava R, Yu C. Electrochemical activity and stability of dealloyed Pt–Cu and Pt–Cu–Co electrocatalysts for the oxygen reduction reaction (ORR). Journal of Power Sources. 2009;**186**:261-267. DOI: https://doi.org/10.1016/j.jpowsour.2008.10.062

[52] Tian N, Zhou Z-Y, Sun S-G. Synthesis of tetrahexahedral platinum nanocrystals with high-index facets and high electro-oxidation activity. Science. 2007;**316**:732-735. DOI: 10.1126/science.1140484

[53] Vitos L, Ruban AV, Skriver HL. The surface energy of metals. Surface Science. 1998;**411**:186-202. DOI: https://doi.org/10.1016/S0039-6028(98)00363-X

[54] Wang C, Hou Y, Kim J. A general strategy for synthesizing FePt nanowires and nanorods. Angewandte Chemie-International Edition. 2007;**46**:6333-6335. DOI: 10.1002/anie.200702001

[55] Zhang N, Feng Y, Zhu X. Superior bifunctional liquid fuel oxidation and oxygen reduction electrocatalysis enabled by PtNiPd core-shell nanowires. Advanced Materials. 2017;**29**. DOI: 10.1002/adma.201603774

[56] Jiang K, Shao Q, Zhao D. Phase and composition tuning of 1D platinum-nickel nanostructures for highly efficient electrocatalysis. Advanced Functional Materials. 2017;**27**. DOI: 10.1002/adfm.201700830

[57] Zhang N, Guo S, Zhu X. Hierarchical Pt/PtxPb core/shell nanowires as efficient catalysts for electrooxidation of liquid fuels. Chemistry of Materials. 2016;**28**:4447-4452. DOI: 10.1021/acs.chemmater.6b01642

[58] Zhang N, Bu L, Guo S. Screw thread-like platinum-copper nanowires bounded with high index facets for efficient electrocatalysis. Nano Letters. 2016;**16**:5037-5043. DOI: 10.1021/acs.nanolett.6b01825

[59] Yang L, Vukmirovic MB, Su D. Tuning the catalytic activity of Ru@Pt core–shell nanoparticles for the oxygen reduction reaction by varying the shell thickness. The Journal of Physical Chemistry C. 2013;**117**:1748-1753. DOI: 10.1021/jp309990e

[60] Oezaslan M, Hasche F, Strasser P. Pt-based core-shell catalyst architectures for oxygen fuel cell electrodes. Journal of Physical Chemistry Letters. 2013;**4**:3273-3291. DOI: 10.1021/jz4014135

[61] Brodsky CN, Young AP, Ng KC. Electrochemically induced surface metal migration in well-defined core–shell nanoparticles and its general influence on electrocatalytic reactions. ACS Nano. 2014;**8**:9368-9378. DOI: 10.1021/nn503379w

[62] Ji M, Li X, Wang H. Versatile synthesis of yolk/shell hybrid nanocrystals via ion-exchange reactions for novel metal/semiconductor and semiconductor/semiconductor conformations. Nano Research. 2017;**10**:2977-2987. DOI: 10.1007/s12274-017-1508-4

[63] Wu Y, Wang D, Li Y. Understanding of the major reactions in solution synthesis of functional nanomaterials. Science China-Materials. 2016;**59**:938-996. DOI: 10.1007/s40843-016-5112-0

[64] Chen Y, Yu Z, Chen Z. Controlled one-pot synthesis of RuCu nanocages and Cu@Ru nanocrystals for the regioselective hydrogenation of quinoline. Nano Research. 2016;**9**:2632-2640. DOI: 10.1007/s12274-016-1150-6

[65] Zhang J, Tang Y, Weng L. Versatile strategy for precisely tailored Core@Shell nanostructures with single shell layer accuracy: The case of metallic shell. Nano Letters. 2009;**9**:4061-4065. DOI: 10.1021/nl902263h

[66] Ji M, Xu M, Zhang W. Structurally well-defined au@Cu2-xS core-shell nanocrystals for improved cancer treatment based on enhanced photothermal efficiency. Advanced Materials. 2016;**28**:3094-3101. DOI: 10.1002/adma.201503201

[67] Huang L, Zheng J, Huang L. Controlled synthesis and flexible self-assembly of mono-disperse Au@semiconductor core/shell hetero-nanocrystals into diverse superstructures. Chemistry of Materials. 2017;**29**:2355-2363. DOI: 10.1021/acs.chemmater.7b00046

[68] Zhang J, Tang Y, Lee K. Nonepitaxial growth of hybrid core-shell nanostructures with large lattice mismatches. Science. 2010;**327**:1634-1638. DOI: 10.1126/science.1184769

[69] Cai S, Hu H, Li H. Design of multi-shell Fe_2O_3@MnOx@CNTs for the selective catalytic reduction of NO with NH_3: Improvement of catalytic activity and SO_2 tolerance. Nanoscale. 2016;**8**:3588-3598. DOI: 10.1039/c5nr08701e

[70] Ghosh T, Vukmirovic MB, DiSalvo FJ. Intermetallics as novel supports for Pt monolayer O-2 reduction electrocatalysts: Potential for significantly improving properties. Journal of the American Chemical Society. 2010;**132**:906. DOI: 10.1021/ja905850c

[71] Xing Y, Cai Y, Vukmirovic MB. Enhancing oxygen reduction reaction activity via Pd−Au alloy sublayer mediation of Pt monolayer electrocatalysts. The Journal of Physical Chemistry Letters. 2010;**1**:3238-3242. DOI: 10.1021/jz101297r

[72] Chen G, Kuttiyiel KA, Su D. Oxygen reduction kinetics on Pt monolayer shell highly affected by the structure of bimetallic AuNi cores. Chemistry of Materials. 2016;**28**:5274-5281. DOI: 10.1021/acs.chemmater.6b00500

[73] Tian X, Tang H, Luo J. High-performance core–shell catalyst with nitride nanoparticles as a core: Well-defined titanium copper nitride coated with an atomic Pt layer for the oxygen reduction reaction. ACS Catalysis. 2017;**7**:3810-3817. DOI: 10.1021/acscatal.7b00366

[74] Deogratias N, Ji M, Zhang Y. Core@shell sub-ten-nanometer noble metal nanoparticles with a controllable thin Pt shell and their catalytic activity towards oxygen reduction. Nano Research. 2015;**8**:271-280. DOI: 10.1007/s12274-014-0664-z

[75] Lee YW, Kim M, Kim ZH. One-step synthesis of Au@Pd core-shell nanooctahedron. Journal of the American Chemical Society. 2009;**131**:17036, 10.1021/ja905603p

[76] Yan J-M, Zhang X-B, Akita T. One-step seeding growth of magnetically recyclable Au@Co core-shell nanoparticles: Highly efficient catalyst for hydrolytic dehydrogenation of ammonia borane. Journal of the American Chemical Society. 2010;**132**:5326. DOI: 10.1021/ja910513h

[77] Feng Q, Zhao S, Wang Y. Isolated single-atom Pd sites in intermetallic nanostructures: High catalytic selectivity for semihydrogenation of alkynes. Journal of the American Chemical Society. 2017;**139**:7294-7301. DOI: 10.1021/jacs.7b01471

[78] Chen M, Tang S, Guo Z. Core-shell Pd@Au nanoplates as theranostic agents for in-vivo photoacoustic imaging, CT imaging, and photothermal therapy. Advanced Materials. 2014;**26**:8210-8216. DOI: 10.1002/adma.201404013

[79] Niu Z, Peng Q, Zhuang Z. Evidence of an oxidative-addition-promoted Pd-leaching mechanism in the Suzuki reaction by using a Pd-nanostructure design. Chemistry—A European Journal. 2012;**18**:9813-9817. DOI: 10.1002/chem.201201224

[80] Yin Z, Lin L, Ma D. Construction of Pd-based nanocatalysts for fuel cells: Opportunities and challenges. Catalysis Science & Technology. 2014;**4**:4116-4128. DOI: 10.1039/c4cy00760c

[81] Koenigsmann C, Sutter E, Adzic RR. Size- and composition-dependent enhancement of electrocatalytic oxygen reduction performance in ultrathin palladium–gold (Pd1–xAux) nanowires. The Journal of Physical Chemistry C. 2012;**116**:15297-15306. DOI: 10.1021/jp306034d

[82] Shao M. Palladium-based electrocatalysts for hydrogen oxidation and oxygen reduction reactions. Journal of Power Sources. 2011;**196**:2433-2444. DOI: 10.1016/j.jpowsour.2010.10.093

[83] Zhang H, Jin M, Xia Y. Enhancing the catalytic and electrocatalytic properties of Pt-based catalysts by forming bimetallic nanocrystals with Pd. Chemical Society Reviews. 2012;**41**:8035-8049. DOI: 10.1039/c2cs35173k

[84] Kondo S, Nakamura M, Maki N. Active sites for the oxygen reduction reaction on the low and high index planes of palladium. The Journal of Physical Chemistry C. 2009;**113**:12625-12628. DOI: 10.1021/jp904278b

[85] Shao M, Yu T, Odell JH. Structural dependence of oxygen reduction reaction on palladium nanocrystals. Chemical Communications. 2011;**47**:6566-6568. DOI: 10.1039/C1CC11004G

[86] Yin Z, Zhou W, Gao Y. Supported Pd–Cu bimetallic nanoparticles that have high activity for the electrochemical oxidation of methanol. Chemistry–A European Journal. 2012;**18**:4887-4893. DOI: 10.1002/chem.201103674

[87] Gao Q, Ju Y-M, An D. Shape-controlled synthesis of monodisperse PdCu nanocubes and their electrocatalytic properties. ChemSusChem. 2013;**6**:1878-1882. DOI: 10.1002/cssc.201300404

[88] Wang Y, Xiong Z, Xia Y. Branched PdAu nanowires with superior electrocatalytic formic acid oxidation activities. RSC Advances. 2017;**7**:40462-40469. DOI: 10.1039/c7ra02115a

[89] Huang JJ, Yang H, Huang QH. Methanol oxidation on carbon-supported Pt-Os bimetallic nanoparticle electrocatalysts. Journal of the Electrochemical Society. 2004;**151**:A1810-A1815. DOI: 10.1149/1.1785932

[90] Saleem F, Ni B, Yong Y. Ultra-small tetrametallic Pt-Pd-Rh-Ag nanoframes with tunable behavior for direct formic acid/methanol oxidation. Small. 2016;**12**:5261-5268. DOI: 10.1002/smll.201601299

[91] Zhang T, Li S-C, Zhu W. Shape-tunable Pt-Ir alloy nanocatalysts with high performance in oxygen electrode reactions. Nanoscale. 2017;**9**:1154-1165. DOI: 10.1039/c6nr08359e

[92] Wu Y-N, Liao S-J, Guo H-F. Ultralow platinum-loading PtPdRu@PtRuIr/C catalyst with excellent CO tolerance and high performance for the methanol oxidation reaction. Rare Metals. 2014;**33**:337-342. DOI: 10.1007/s12598-013-0063-8

[93] Masatake H, Tetsuhiko K, Hiroshi S. Novel gold catalysts for the oxidation of carbon monoxide at a temperature far below 0°C. Chemistry Letters. 1987;**16**:405-408. DOI: 10.1246/cl.1987.405

[94] Yin H, Tang H, Wang D. Facile synthesis of surfactant-free Au cluster/graphene hybrids for high-performance oxygen reduction reaction. ACS Nano. 2012;**6**:8288-8297. DOI: 10.1021/nn302984x

[95] Xu H, Yan B, Wang J. Self-supported porous 2D AuCu triangular nanoprisms as model electrocatalysts for ethylene glycol and glycerol oxidation. Journal of Materials Chemistry A. 2017;**5**:15932-15939. DOI: 10.1039/c7ta04598k

[96] Tammeveski L, Erikson H, Sarapuu A. Electrocatalytic oxygen reduction on silver nanoparticle/multi-walled carbon nanotube modified glassy carbon electrodes in alkaline solution. Electrochemistry Communications. 2012;**20**:15-18. DOI: 10.1016/j.elecom.2012.04.003

[97] Gupta RK, Verma AD, Sinha I. Oxygen reduction reaction on anisotropic silver nanoparticles in alkaline media. Chemical Physics Letters. 2017;**680**:6-9. DOI: 10.1016/j.cplett.2017.05.031

[98] Zheng J, Zhuang Z, Xu B. Correlating hydrogen oxidation/evolution reaction activity with the minority weak hydrogen-binding sites on Ir/C catalysts. ACS Catalysis. 2015;**5**:4449-4455. DOI: 10.1021/acscatal.5b00247

[99] Qin B, Yu H, Chi J. A novel Ir/CeO2-C nanoparticle electrocatalyst for the hydrogen oxidation reaction of alkaline anion exchange membrane fuel cells. RSC Advances. 2017;**7**:31574-31581. DOI: 10.1039/c7ra03675b

[100] Lin C, Wu G, Li H. Rh nanoparticles supported on ultrathin carbon nanosheets for high-performance oxygen reduction reaction and catalytic hydrogenation. Nanoscale. 2017;**9**:1834-1839. DOI: 10.1039/c6nr09739a

[101] Cao DX, Wieckowski A, Inukai J. Oxygen reduction reaction on ruthenium and rhodium nanoparticles modified with selenium and sulfur. Journal of the Electrochemical Society. 2006;**153**:A869-A874. DOI: 10.1149/1.2180709

[102] Zaikovskii VI, Nagabhushana KS, Kriventsov VV. Synthesis and structural characterization of Se-modified carbon-supported ru nanoparticles for the oxygen reduction reaction. Journal of Physical Chemistry B. 2006;**110**:6881-6890. DOI: 10.1021/jp056715b

[103] Neergat M, Gunasekar V, Singh RK. Oxygen reduction reaction and peroxide generation on Ir, Rh, and their selenides—A comparison with Pt and RuSe. Journal of the Electrochemical Society. 2011;**158**:B1060-B1066. DOI: 10.1149/1.3604744